Electron-energy-loss near-edge structures in the oxygen K-edge spectra of transition-metal oxides

H. Kurata,* E. Lefèvre, and C. Colliex
Laboratoire de Physique des Solides, Bâtiment 510, Université Paris-Sud, 91405 Orsay CEDEX, France

R. Brydson
Department of Materials Science and Engineering, University of Surrey, Guildford, Surrey GU2 5XH, United Kingdom
(Received 27 October 1992)

Oxygen K-edge electron-energy-loss spectra have been recorded for several transition-metal oxides (NiO, MnO, MnO_2, TiO_2, Cr_2O_3, Mn_2O_3) of different crystal structures. The origin of the distinct features which can be identified over 40 eV above threshold is discussed in terms of resonance scattering within shells of neighboring anionic backscatterers. Full multiple-scattering calculations corroborate and correct the simple approach. The first peak at threshold is due to transitions to oxygen $2p$ states hybridized with the narrow metal $3d$ band which is highly localized around the metal-atom sites. The other near-edge structures are dominated by the arrangement of oxygen anions around the excited central atom.

I. INTRODUCTION

Fine structures on core-excitation electron-energy-loss spectra provide a wealth of information about the local electronic structure as well as the crystal environment of the excited atom. This information is very diverse and reflects different kinds of neighborhoods depending on the energy-loss range under consideration. The fine structures can be roughly divided into strong oscillations up to 30–50 eV above threshold, usually called near-edge structure (ELNES for energy-loss experiments and XANES for x-ray-absorption measurements), and weaker oscillations, from 30 to 50 eV up to several hundred eV, often designated as EXELFS (extended energy-loss fine structure) or EXAFS (extended x-ray-absorption fine structure).

In the present work, we have investigated the oxygen K-edge ELNES of several simple transition-metal oxides which are typical of different crystal structures, i.e., monoxides (NiO and MnO) are of NaCl-type structure, dioxides (MnO_2 and TiO_2) are of rutile structure, and Mn_2O_3 is of bixbyite structure. Our purpose is to identify the origin of the different features observed in these spectra by monitoring the modifications associated with changes in coordination and valence state. In the last few years, it has actually been demonstrated that the ELNES structure is governed by the arrangement and type of atoms in the first coordination shell, a so-called "coordination fingerprint."[1,2] In fact, this statement must be refined. Electron-energy-loss excitation, as in x-ray absorption, is a local process in which an electron is promoted to an excited electronic state, which can be coupled to the original core level through the dipole selection rule ($\Delta l = \pm 1$) if the momentum transfer upon excitation is small. Consequently, an oxygen K edge must display, in the first approximation, the distribution of the oxygen p-projected unoccupied density of states. For these samples, we shall show that this edge can actually be divided into two regions. In the first 5–10 eV from the threshold, the oxygen $2p$ character is hybridized with the transition-metal $3d$ levels,[3,4] and de Groot *et al.*[5] have analyzed in detail the recorded spectral features in terms of ligand-field and exchange splittings. In the second region, i.e., from 5 or 10 eV to about 30 eV, the O $2p$ character is hybridized with the weakly structured metallic $4sp$ band and constitutes a kind of accessible continuum state. Band-structure-calculation results[5] on CuO with extended basis sets, i.e., including also metal $4s$ and $4p$ and oxygen $3s$ and $3p$ states, show that the energy region up to 15 eV above the Fermi level is predominantly of O $2p$ character (not O $3p$). Consequently, the oscillations recorded in this energy range do not correspond to transitions towards bound states but to interference effects resulting from multiple scattering of the excited electron by neighboring atoms. They are therefore rather sensitive to structural parameters.

The interpretation of these structures is still the subject of some controversy. In several cases, such as in molecular species, it has been shown that certain ions (i.e., O^{2-}) are strong backscatterers and can give rise to potential cages or barriers for electron scattering.[6] Resonance effects then occur with a clear correlation between the energy position of the resonance peak above threshold (ΔE) and the distance (R) between the excited atom and the backscattering cage:[7]

$$\Delta E R^2 = \text{constant} . \quad (1)$$

A number of studies have been published to support this correlation, and in particular the metal K absorption edge in transition-metal oxides has been interpreted using Eq. (1).[6–10] The present paper will discuss how our experimental ELNES features can be interpreted in terms of resonance scattering, as compared to the results of the full multiple-scattering theory.[11,12]

II. EXPERIMENTAL RESULTS

The electron-energy-loss-spectroscopy (EELS) spectra have been recorded with a VG-STEM electron microscope equipped with a field-emission source and a Gatan-parallel EELS spectrometer.[13] The energy resolution is of the order of 0.8 eV in the oxygen K-edge region at around 530 eV. In order to reduce the effects of multiple-loss events which can induce artifacts and extra contributions in the involved energy-loss domain (i.e., between 20 and 30 eV above threshold), the raw data have been deconvoluted by low loss spectra measured under similar conditions on the same specimen area.

Figure 1 shows the oxygen K-edge ELNES after background subtraction for the monoxides and dioxides. Four main peaks are identified on each spectrum ($a-d$), the positions of which are listed in Table I.

Peaks labeled a correspond to the first type of excitation described above, i.e., to transitions towards p-d hybridized vacant states. The relative weight of this contribution, as compared to the total intensity of the K edge, increases monotonically from NiO to MnO, MnO_2, and TiO_2. This reflects the increased number of accessible vacant d states along this sequence.

The following peaks, labeled $b-d$, will be analyzed in detail in the present paper. They constitute the ELNES contribution and their distribution is governed by scattering effects from the surrounding shells. Davoli *et al.*[14] have already pointed out the similarity of all multiple-scattering peaks ($b-d$ in the present terminology) in the O K spectra of NiO and MgO, which reflects the same local atomic environment in both oxides. The lack of peak a in MgO (see Colliex[15]) confirms that its presence in NiO has to be associated with the existence of unoccupied states made of mixed O-2p orbitals with Ni-3d orbitals. These authors also demonstrate that the one-electron full multiple-scattering theory cannot account for the origin of two weak structures marked by an asterisk in Fig. 1. They discuss the possibility of mixing of final-state configurations as giving rise to these extra features. We can also confirm that these peaks do not come from multiple-loss events because we have performed the deconvolution of lower loss components.

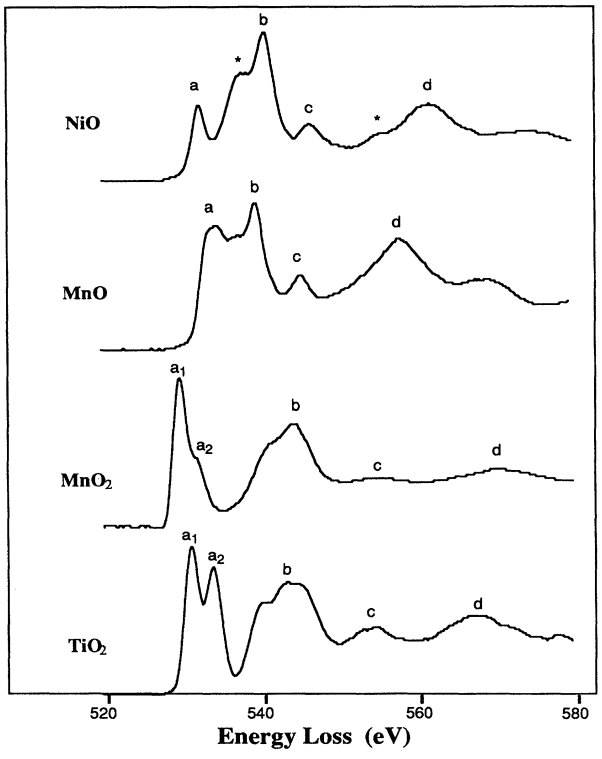

FIG. 1. Experimental O K-edge spectra from transition-metal monoxides and dioxides after deconvolution of multiple-loss events and subtraction of background.

TABLE I. Energy position (in eV) for the major features identified over the ELNES energy domain of the O K edges displayed in Fig. 1.

eV	NiO	MnO	MnO_2	TiO_2
aa_1	531.7	533.8	529.0	530.7
a_2			531.0	533.4
b	540.1	539.1	543.5	543.0
c	546.0	544.8	553.8	554.1
d	561.2	557.5	569.6	567.0

III. DISCUSSION OF THE RESULTS

Detailed multiple-scattering (MS) calculations have been performed for the oxygen K-edge ELNES of MgO by Lindner *et al.*[16] and of MgO, CaO, and SrO by Weng and Rez.[17] In particular, when considering the origin of the different fine structures as a function of the size of the cluster shell, their calculations demonstrate that the backscattering by the successive oxygen shells dominates the ELNES features because of the larger backscattering of oxygen anions compared to that of metal cations over the energy range of ELNES. As a result, it was suggested that peaks (d) and (c) in the MgO case should be attributed to a single scattering, respectively, from the nearest-neighbor oxygen shell (second shell around the excited atom) and the second oxygen shell (fourth shell around the excited atom).[18,19] It is therefore interesting to investigate how far this simple interpretation of the oxygen K-edge ELNES can be confirmed and extended to transition-metal oxides. For that purpose we shall compare the theoretical results of full multiple-scattering calculations with simple arguments in terms of resonance scattering.

The full multiple-scattering calculations have been performed using the ICXANES computer code of Vvedensky and Pendry[11] and Vvedensky, Saldin, and Pendry.[12] Scattering phase shifts and atomic matrix elements were obtained by imposing a muffin-tin potential on the structure of MnO. Muffin-tin radii were chosen to be $r_{Mn}=2.2371$ a.u. (1 a.u.$=0.529\,18$ Å) and $r_0=1.9543$ a.u. since this minimizes the discontinuity in potential at the boundaries of the muffin tins. The effects of charge transfer, via use of a Madelung-type correction, were not explicitly included. The core hole was accounted for by

the use of the $(Z+1)^*$ approximation for the central oxygen atom in the cluster. Phase shifts up to $l=3$ were employed and the damping term was adjusted to provide reasonable agreement with experiment (this was of the order of 1 eV). The energy scales of the final (i.e., full shell) calculated spectra were all adjusted to agree with experiment via use of a compression factor equal to 0.87. This is very similar to the one employed by Davoli *et al.*[14] in their comparison of the theory of Vvedensky and Pendry and Vvedensky, Saldin, and Pendry with the O K XANES of NiO and arises due to a neglect of the energy dependence of the exchange interaction.

On the other hand, one can examine how the resonance condition expressed in Eq. (1) can be used within this context. Following the above argument, it is supposed that the peak positions are sensitive to the interatomic distances between oxygen atoms. Therefore, in order to eliminate the effects in the spectrum arising from the different interatomic distances, we have rescaled the energy axis in Fig. 2 by a factor $(R/R_{\text{ref}})^2$, where R_{ref} is the first-neighbor O-O distance in NiO and R is the corresponding value for each oxide. Rescaled spectra are aligned with each other by fixing the binding energy of the O-1s level relative to the Fermi level deduced from the XPS measurements.[20] We observe a satisfactory alignment of peaks b and d in all spectra in spite of the different local structure around the oxygen atom in the NaCl- and rutile-type structures and the different metal ions. This fact confirms that the main contributions for peaks b and d are due to backscattering from the oxygen shells. Then we can attribute peaks b and d, respectively, to intrashell multiple scattering and to single scattering within the first shell of neighboring oxygen atoms. In Fig. 3 we have plotted the resonance energy of peak d relative to the Fermi level versus $1/R^2$. It is clear that energy positions of peak d follow a linear dependence with $1/R^2$.

Let us now consider for each investigated specimen how the full multiple-scattering-calculation data fit with the simplified resonance arguments. First of all, the ICXANES results confirm that the dominant scatterers in these oxide structures are the oxygen atoms and/or ions and it is almost possible to reproduce many of the basic spectral features using a cluster absent of the metal atoms and/or ions.

A. MnO

Reasonable agreement is achieved with a cluster consisting of seven shells (cluster radius $=11.86$ a.u.), as visible in Fig. 4. By varying the cluster size (see Fig. 5), the following assignments can be proposed for the features in the experimental spectrum.

(i) *Peak a.* The basic structure in this region is reproduced by using solely the first coordination shell of manganese. The dominant scattering events are d-like scattering from Mn and p-like scattering from oxygen. Hence this feature reflects transitions to oxygen $2p$ states hybridized with the narrow metal $3d$ band which is highly localized around the metal-atom sites. The fine details (notably the features lying between peaks a and b) are

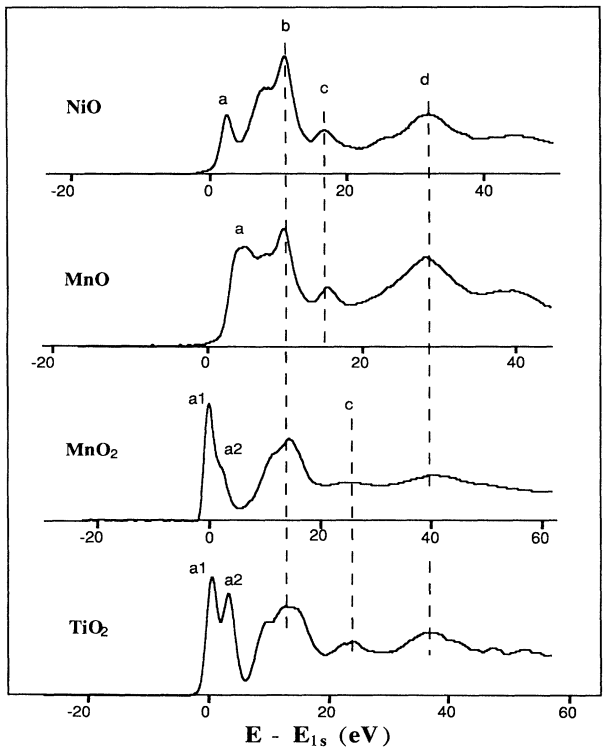

FIG. 2. The same oxygen K-edge ELNES spectra after scaling for comparison. The energy axis has been rescaled by a factor $(R/R_{\text{ref}})^2$, where R_{ref} is the first-neighbor O-O distance in NiO and R is the corresponding values for each oxide. The zero of energy corresponds to the Fermi level deduced from XPS measurements.

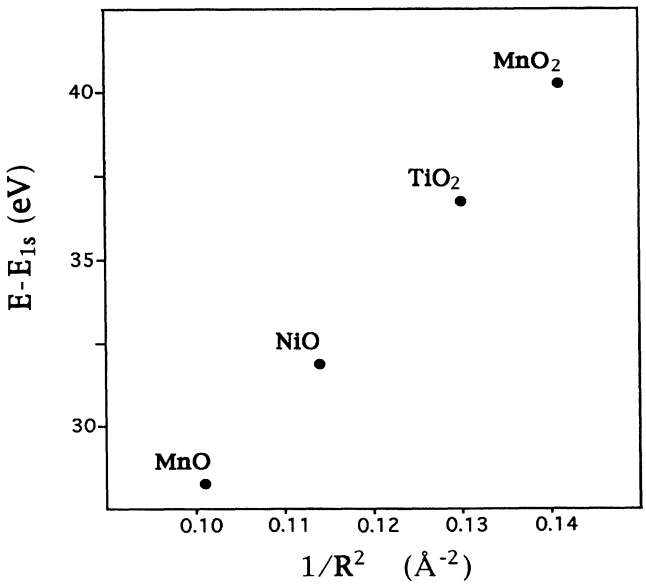

FIG. 3. Plot of the energy of the resonance peak (d) energy in Fig. 2 vs $1/R^2$.

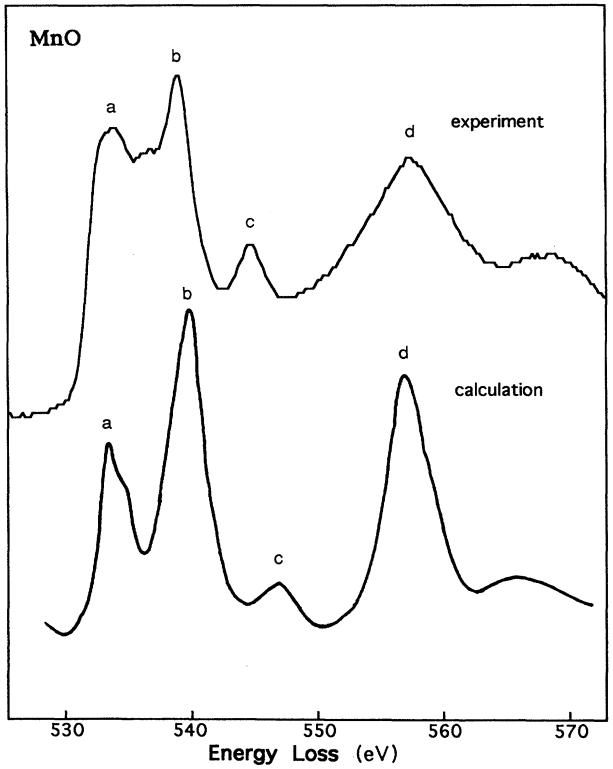

FIG. 4. Comparison of the experimental and MS-calculated oxygen K-edge ELNES spectra for MnO.

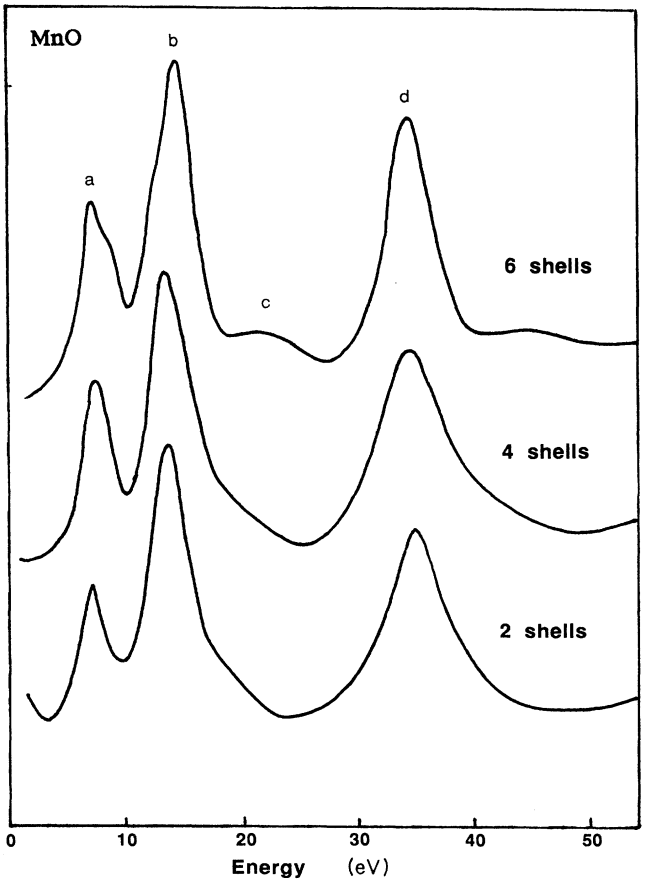

FIG. 5. MS calculation of the oxygen K-edge ELNES spectra in MnO for different numbers of shells surrounding the exited atom.

only reproduced after addition of a third oxygen coordination shell, indicating that this region is also sensitive to long-range effects.

(ii) *Peak b.* This feature reflects transitions to oxygen $2p$ states hybridized with the more-delocalized transition-metal $4s$ and $4p$ states. In terms of scattering, the exact structure arises from intrashell multiple scattering within the first oxygen coordination shell—this is in agreement with the findings of Vvedensky and Pendry[11] on NiO and Rez, Weng, and Ma[18] on MgO.

(iii) *Peak c.* This feature (and the feature lying to the higher-energy-loss side of peak d) seems to be only reproduced after addition of a third oxygen coordination shell. The modification in Fig. 5 between the four shell and the two shell curves, if there is one, is less important than between the six shell and the four shell curves. It therefore arises mainly from intershell multiple scattering. In the simplified resonance scattering model, this peak (c) remains almost at a fixed energy position if the local structure is the same but shifts if the environment is modified. In the monoxides the energy of peak c is about half that of peak d. Since the resonance energy is proportional to $1/R^2$, peak c could then be attributed to single scattering from the second neighboring oxygen shell, the distance of which is $\sqrt{2}$ times as long as the first-neighbor O-O distance in NaCl structure, which would be consistent with the assignment for the oxygen K-edge of MgO.[18,19] The full MS calculations are in conflict with this simple conclusion.

(iv) *Peak d.* This feature is reproduced using the first oxygen coordination shell and arises from dominantly single-scattering events from this shell, as suggested by the simple resonance scattering arguments.

B. MnO_2

Reasonable agreement is achieved with an eight-shell cluster (cluster radius $=10.43$ a.u.) (Fig. 6). The shell structure is considerably more complex than in the case of the rocksalt structure due to the lower symmetry at the oxygen site. However, the following general assignments can be concluded.

(i) *Peak a* has basically the same origin as peak a in MnO, although the number of transition-metal nearest neighbors has decreased from six to three.

(ii) *Peak b* has basically the same origin as peak b in MnO, intrashell multiple scattering within the first oxygen coordination shell. The additional structure on both the low- and high-energy sides of the main peak b arises when the second oxygen coordination shell is included.

(iii) *Peak c* arises from outer-lying (not first or second) oxygen coordination shells and involves intershell multiple scattering. It perhaps explains why the relative posi-

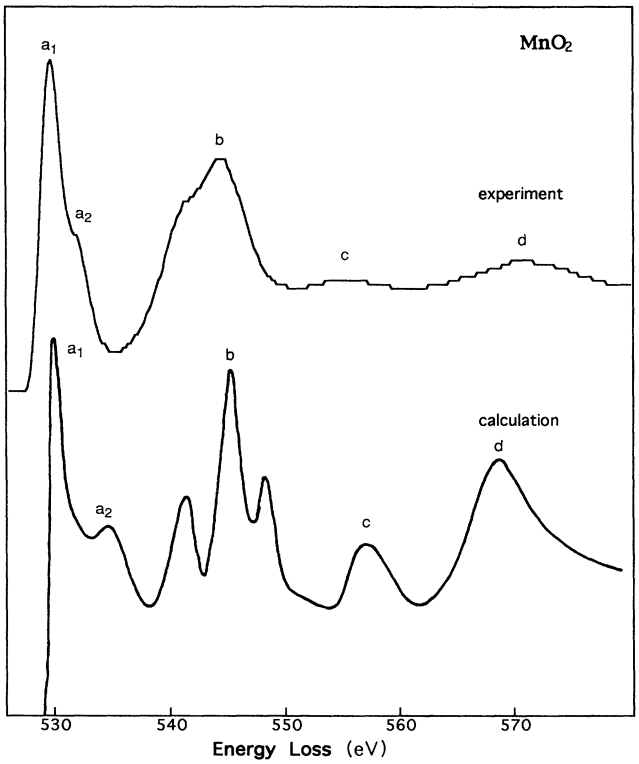

FIG. 6. Comparison of the experimental and MS-calculated oxygen K-edge ELNES spectra for MnO_2

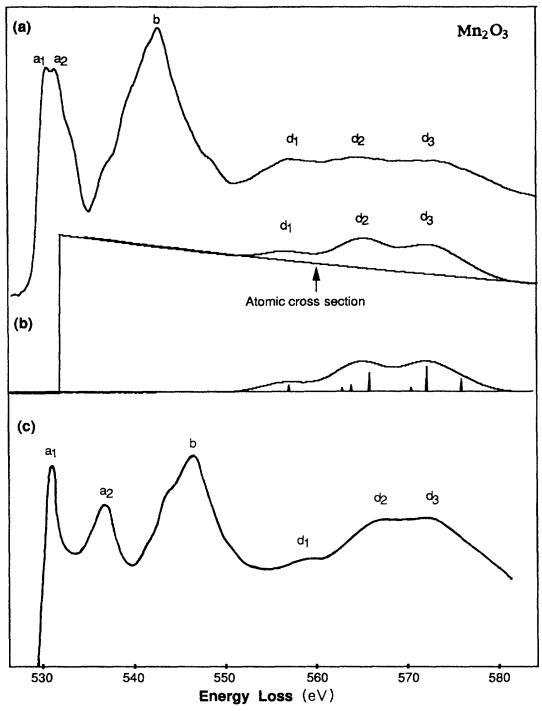

FIG. 7. ELNES spectra of oxygen K edge for Mn_2O_3. (a) Experimental, (b) simplified calculation assuming single scattering from the first surrounding shell of oxygen atom, (c) full multiple-scattering (MS) calculation.

tion of this feature is sensitive to the structure type (e.g., rocksalt or rutile type) since its origin is somewhat more complex and depends on the relative arrangements of the different shells.

(iv) *Peak d* has the same origin as peak *d* in MnO and is due to single scattering from the nearest-neighbor oxygen shell. It confirms that the relationship $\Delta E \propto 1/R^2$ is applicable to the energy position of this feature for both the rocksalt- and rutile-type oxide structures.

These results may be logically extended to the O K edge of TiO_2 rutile. A previous multiple-scattering calculation without compression of the energy scale is contained in Ref. 21.

C. Mn_2O_3

Reasonable agreement is achieved with a seven-shell cluster [cluster radius $=9.90$ a.u. (Ref. 22)] [Fig. 7(c)]. This is of very low symmetry and hence the calculation is expected to be less accurate.

(i) *Peak a* has basically the same origin as peak *a* in MnO and Mn_2O_3 although the number of transition-metal nearest neighbors is four.

(ii) *Peak b* seems to result from intrashell multiple scattering within the first oxygen shell as in the case of MnO and MnO_2.

(iii) *Peak d* is split into three peaks (d_1, d_2, and d_3) that are due to single scattering from the first oxygen coordination shell, which contains seven different O-O distances, confirming therefore the validity of the resonance scattering conditions even in such complex cases. As there are several (7) different first-neighbor distances in the unit cell, a number of resonance peaks associated with single scattering from the first oxygen shell are expected. Figure 7 compares the experimental O K-shell ELNES structure where three peaks (d_1, d_2, and d_3) are easily discernable [Fig. 7(a)] with a simple calculation using the resonance condition [Fig. 7(b)]. Since peak *d* arises from resonance scattering between the central oxygen atom and its nearest-neighbor oxygen atoms, the constant value in Eq. (1) can be assumed to be identical in all cases of interest. It has therefore been estimated from the slope of the line in Fig. 3. The interatomic distances were derived from the crystal structure. The vertical bars in Fig. 7 represent the calculated resonance peak positions. In order to compare with the experimental spectrum, they have been convoluted with a Gaussian curve of width 6 eV and the intensities have been weighted by a $1/E$ factor to take account of the attenuation of the excitation probability. The calculated resonance spectra have then been added to the atomic cross section of the oxygen K edge, which was calculated using the SIGMAK program.[23] The calculated resonance spectra are in good agreement with the experimental ones, emphasizing the justification of the assignment of peak *d*.

It must be pointed out that in order to get a best fit between calculated spectra and experimental ones, the calculated spectrum needs be shifted to higher energy by 5 eV for Mn_2O_3. The energy shift may be related to the definition of the zero of energy. In multiple-scattering

theory[24] the energy of resonance peaks is referenced to the "muffin-tin zero potential." However, this value is experimentally inaccessible. In this work we have defined the resonance energy with respect to the Fermi level. In fact, the linear correlation between ΔE and $1/R^2$ shown in Fig. 3 indicates that the muffin-tin zero value relative to the Fermi level is almost constant in monoxides and dioxides. Similar results have been found in chemisorbed molecular systems.[25] But in the case of Mn_2O_3, the muffin-tin zero seems to be different from that of monoxides and dioxides. For a more quantitative understanding, the full MS calculation showing the weight of multiple scattering contributions from each shell was therefore required.

IV. CONCLUSION

The oxygen K ELNES's of several simple transition-metal oxides have been analyzed in terms of scattering theory. Via the use of simple comparisons between structure types and the results of full multiple-scattering theory, we have shown that the near-edge structure is dominated by the arrangement of oxygen anions around the central atom. Features corresponding to scattering resonances from the nearest-neighbor oxygen shell have been identified and their energy dependence has been confirmed as varying as the inverse square of the distance.

Such an analysis has been extended to the more-complicated case of the bixbyite structure, which contains a range of differing distances within the first oxygen shell. In principle it should be possible to use this technique to determine the relative degree of disorder in an unknown oxide structure.

ACKNOWLEDGMENTS

One of the authors (H.K.) is grateful to the Centre National de la Recherche Scientifique (CNRS) for providing financial support during this work.

*Permanent address: Institute for Chemical Research, Kyoto University, Uji, Kyoto 611, Japan.

[1]R. Brydson, H. Sauer, W. Engel, J. M. Thomas, and E. Zeitler, J. Chem. Soc. Chem. Commun. **15**, 1010 (1989).

[2]R. Brydson, H. Sauer, and W. Engel, in *Transmission Electron Energy Loss Spectrometry in Materials Science,* edited by M. M. Disko, C. C. Ahn, and B. Fultz (The Minerals, Metals & Materials Society, Warrendale, PA 1992), p. 131.

[3]L. A. Grunes, R. D. Leapman, C. N. Wilker, R. Hoffmann, and A. B. Kunz, Phys. Rev. B **25**, 7157 (1982).

[4]C. Colliex, T. Manoubi, and C. Ortiz, Phys. Rev. B **44**, 11 402 (1991).

[5]F. M. F. de Groot, M. Grioni, J. C. Fuggle, J. Ghijsen, G. A. Sawatzky, and H. Petersen, Phys. Rev. B **40**, 5715 (1989); M. Grioni, M. T. Czyzyk, F. M. F. de Groot, J. C. Fuggle, and B. E. Watts, *ibid.* **39**, 4886 (1989).

[6]A. Bianconi, M. Dell'Ariccia, P. J. Durham, and J. B. Pendry, Phys. Rev. B **26**, 6502 (1982).

[7]A. Bianconi, M. Dell'Ariccia, A. Gargano, and C. R. Natoli, in *EXAFS and Near-Edge Structure,* edited by A. Bianconi, L. Incoccia, and S. Stipcich (Springer-Verlag, Berlin, 1983), p. 57.

[8]R. N. Sinha, P. Mahto, and A. R. Chetal, Z. Phys. B **81**, 229 (1990).

[9]A. Bianconi, E. Fritsch, G. Calas, and J. Petiau, Phys. Rev. B **32**, 4292 (1985).

[10]F. W. Lytle and R. B. Greegor, Phys. Rev. B **37**, 1550 (1988).

[11]D. D. Vvedensky and J. B. Pendry, Phys. Rev. Lett. **54**, 2725 (1985).

[12]D. D. Vvedensky, D. K. Saldin, and J. B. Pendry, Comput. Phys. Commun. **25**, 193 (1982).

[13]D. Bouchet, C. Colliex, P. Flora, O. Krivanek, C. Mory, and M. Tencé, Microsc. Microanal. Microstruct. **1**, 443 (1990).

[14]I. Davoli, A. Marcelli, A. Bianconi, M. Tomellini, and M. Fanfoni, Phys. Rev. B **33**, 2979 (1986).

[15]C. Colliex, Adv. Opt. Electron Microsc. **9**, 65 (1984).

[16]Th. Lindner, H. Sauer, W. Engle, and K. Kambe, Phys. Rev. B **33**, 22 (1986).

[17]X. Weng and P. Rez, Phys. Rev. B **39**, 7405 (1989).

[18]P. Rez, X. Weng, and H. Ma, Microsc. Microanal. Microstruct. **2**, 143 (1991).

[19]T. Manoubi, Thesis of Doctorat d'Etat, Orsay, 1989; C. Colliex, in *Transmission Electron Energy Loss Spectrometry in Materials Science* (Ref. 2), p. 85.

[20]C. N. R. Rao, D. D. Sarma, S. Vasudevan, and M. S. Hegde, Proc. R. Soc. London, Ser. A **367**, 239 (1979).

[21]R. Brydson, H. Sauer, W. Engel, E. Zeitler, J. M. Thomas, N. Kosugi, and H. Kuroda, J. Phys. Condens. Matter. **1**, 797 (1986).

[22]S. Geller, Acta Crystallogr. Sec. B **27**, 821 (1971).

[23]R. F. Egerton, *Electron Energy-Loss Spectroscopy in the Electron Microscope* (Plenum, New York, 1986).

[24]C. R. Natoli, in *EXAFS and Near-Edge Structure* (Ref. 7), p. 43.

[25]J. Stöhr, J. L. Gland, W. Eberhardt, D. Outka, R. J. Madix, F. Sette, R. J. Koestner, and U. Doebler, Phys. Rev. Lett. **51**, 2414 (1983).